This article was downloaded by:[Godfrey, Thomas A.]
On: 28 January 2008
Access Details: [subscription number 790010776]
Publisher: Taylor & Francis
Informa Ltd Registered in England and Wales Registered Number: 1072954
Registered office: Mortimer House, 37-41 Mortimer Street, London W1T 3JH, UK

Journal of the Textile Institute
Publication details, including instructions for authors and subscription information:
http://www.informaworld.com/smpp/title~content=t778164490

A micromechanical model for extension of a tightly packed bundle of aligned short fibres

Thomas A. Godfrey [a]
[a] Natick Soldier Center, U.S. Army Research Development & Engineering Command, Natick, MA

Online Publication Date: 01 April 2008
To cite this Article: Godfrey, Thomas A. (2008) 'A micromechanical model for extension of a tightly packed bundle of aligned short fibres', Journal of the Textile Institute, 99:2, 101 - 109
To link to this article: DOI: 10.1080/00405000701489768
URL: http://dx.doi.org/10.1080/00405000701489768

PLEASE SCROLL DOWN FOR ARTICLE

Full terms and conditions of use: http://www.informaworld.com/terms-and-conditions-of-access.pdf

This article maybe used for research, teaching and private study purposes. Any substantial or systematic reproduction, re-distribution, re-selling, loan or sub-licensing, systematic supply or distribution in any form to anyone is expressly forbidden.

The publisher does not give any warranty express or implied or make any representation that the contents will be complete or accurate or up to date. The accuracy of any instructions, formulae and drug doses should be independently verified with primary sources. The publisher shall not be liable for any loss, actions, claims, proceedings, demand or costs or damages whatsoever or howsoever caused arising directly or indirectly in connection with or arising out of the use of this material.

Downloaded By: [Godfrey, Thomas A.] At: 13:54 28 January 2008

Taylor & Francis
Taylor & Francis Group

A micromechanical model for extension of a tightly packed bundle of aligned short fibres

Date Submitted 15 March 2006, Date Accepted 16 October 2006 doi:10.1080/00405000701489768

Thomas A. Godfrey

Natick Soldier Center, U.S. Army Research Development & Engineering Command, Natick, MA 01760-5020

Abstract: Micromechanical models for the interaction between discrete short fibres in idealized bundles are developed and are used to investigate fibre strain profiles, slippage behaviour with increasing extension, bundle load-extension, and tangent stiffness properties. The modeling approach permits abutting fibres to interact by elastic surface shear forces in gripping regions and inelastic frictional slip in slipping regions, where transition from gripping to slipping at a contact position occurs as a linear elastic–perfectly plastic function of the interfibre relative displacement. Results show that for typical staple fibre dimensions and physical properties, a short fibre composite model for the fibre strain profile provides a good approximation to the average fibre strain profile occurring along fibres embedded in bundles. For one fibre assembly considered, results for bundle tangent stiffness indicate that, with increasing extension, average bundle stiffness may be expected to decrease from about 0.8 to 0.5 relative to a bundle of similar but continuous fibres, with 0.5 being reached at the point of collapse by localized slippage.

Key words: Fibre bundle, staple yarn, slippage, friction, theoretical model, stiffness

INTRODUCTION

An elusive goal of many textile mechanics studies has been to relate the tensile extension behaviour of staple yarns to the properties of the constituent fibres and the detailed structural geometry of the yarn. Generally, *micromechanical* models or assumptions are used to treat the effect of fibre discontinuities and interfibre slip and define the resulting stress profile along fibres. A yarn structural model is then used to determine the yarn load by integrating the fibre stresses over the yarn cross section, taking into account the distribution of fibres in the yarn and the orientation or obliquity effect due to twist. Due to the overall complexity of the task, only the simplest assumptions are made at the micromechanical level regarding the interactions between neighbouring fibres. In the present work, the interactions between discrete aligned short fibres in an idealized bundle are examined in-depth. The interface between abutting fibres is assumed to be partially slipping and partially gripping, with slipping regions occurring near fibre tips. The growth of slipping regions with increasing bundle extension is investigated and is used to elucidate the self-locking behaviour of staple yarns. Results for the load-extension behaviour of the idealized bundle provide an insight into the relationship between fibre elastic properties and the tangent stiffness of bundles of short fibres.

The simplest and most commonly used model for the interaction of an individual staple fibre with neighbours within a fibrous assembly structure results from treating the surrounding fibres as a homogeneous medium and assuming that the fibre slips relative to the medium in regions near the fibre tips. All load transfer, occurring through surface frictional shear stresses, is assumed to occur within the slipping regions. The model and associated fibre surface shear and axial stresses are exhibited in Figure 1 (reproduced from Shao *et al.* 2005). Shao and coworkers refer to this model as the *short fibre composite model* (because of its correspondence to an isolated fibre in a matrix) and use it successfully in a comprehensive modeling approach to predict yarn strength, load-extension curves, and cyclic response. It is essentially the same simple model adopted by Hearle (1965) to analyze the mechanics of twisted staple yarns; Hearle provides an enhanced exposition of the model in a book chapter (Hearle, 1989, pp. 40–43). An aim of the present work is to examine fibre interactions and the relationship between macroscopic and microscopic behaviour seen in idealized bundles of discrete short fibres and compare with the extreme case of averaging represented by the short fibre composite model. It will be shown that the short fibre composite model provides a good approximation for the behaviour of bundles of short fibres under realistic assumptions about fibre properties and bundle geometry.

Corresponding Author:
T. A. Godfrey
Natick Soldier Center
U.S. Army Research Development & Engineering Command
Natick, MA 01760-5020
[redacted]

Copyright © 2008 The Textile Institute

Downloaded By: [Godfrey, Thomas A.] At: 13:54 28 January 2008

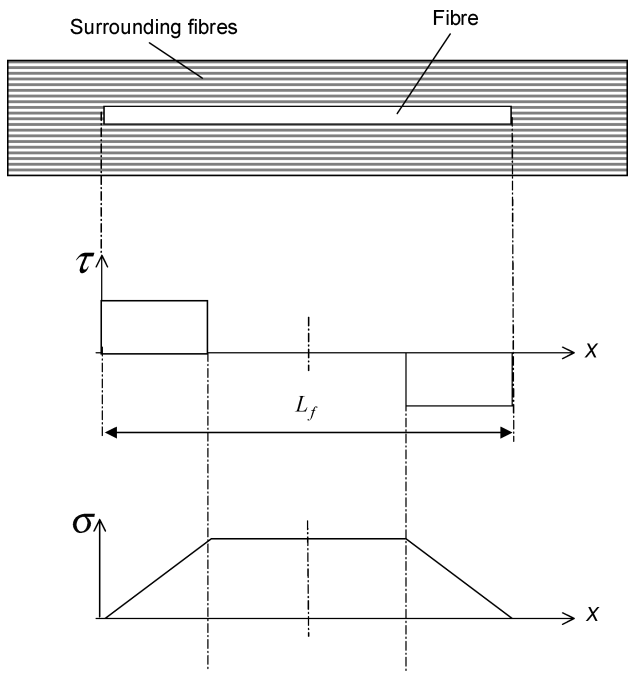

Figure 1 A composite model to represent a fibre in staple yarn and stress distribution along the fibre.

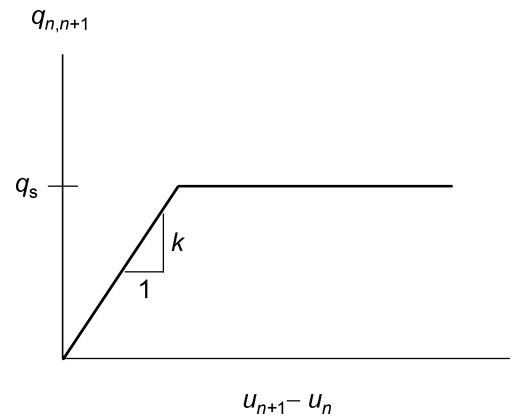

Figure 2 Constitutive behaviour of interfibre contact line shear traction.

MODELING GRIPPING AND SLIPPING INTERACTIONS BETWEEN FIBRES

In order for a bundle of fibres to remain *locked*, relative motion or slip between fibres must be inhibited to a degree. Fibre-to-fibre interfaces may be partially slipping, but an appropriate network of gripping locations must exist to prevent drafting of the bundle. Fibres that slip completely along their length carry tension due to frictional slip tractions; however, the development of large slip displacements between the fibre and its neighbours is not inhibited, and the fibre may pull out of the bundle.

We consider a tightly packed bundle of perfectly aligned short fibres. As such, the idealized bundle is not intended to faithfully represent the local arrangement of fibres in real fibrous assemblies, where the complicating factors of fibre crimp, misalignment, entanglements, and, in twisted yarns, migration, are present to greater or lesser degrees. The emphasis here is on bringing out the effects of interactions between discrete fibres, where the only concession to the presence of the overall fibrous structure in which the bundle is embedded is the assumption of a simple uniform lateral pressure consolidating the bundle. Although the bundles modeled here are highly idealized, we envision the assumed configurations as a fair approximation to conditions at the core of a ring-spun cotton or polyester yarn, where we may expect a coherent structure with a high-fibre packing density (Goswami *et al.*, 1991).

The coordinate x gives the position of points along the axis of the fibre bundle. The bundle is quasi-statically extended such that, at a given instant, the nominal or average strain of the bundle is ε_0. If the bundle is considered to be a portion of a twisted yarn, bundle extension arises from extension of the yarn in which it is embedded and is accompanied by increasing lateral stress due to yarn twist. The average axial displacement of points on the nth fibre is denoted $u_n = u_n(x)$. Suppose fibres n and $n+1$ abut in a region $x^{(1)} \leq x \leq x^{(2)}$. A shear traction of $q_{n,n+1}(x)$, with dimension of force/length, is exerted on fibre n by fibre $n+1$ along the contact line, where $q_{n,n+1}(x)$ acts in the positive x direction for $u_{n+1} > u_n$. For gripping contact in the region $x^{(1)} \leq x \leq x^{(2)}$, we assume (Godfrey and Rossettos, 2001) that the shear traction is proportional to the difference in average displacement of the two abutting fibres, written as

$$q_{n,n+1} = k(u_{n+1} - u_n). \tag{1}$$

The proportionality factor k is interpreted as an elastic constant representing shearing of the abutting fibres along the contact line. We assume shear traction is limited by the "frictional strength" of the contact, where the overall behaviour may be regarded as elastic-perfectly plastic, as illustrated in Figure 2. For slipping contact, the shear traction takes the limiting value q_s. Differences between static and kinetic friction are neglected.

Specific regions along the contact line between two abutting fibres may be gripping or slipping at a given instant in the extension process. Generally, as will be shown later, slipping regions tend to grow with increasing extension at the expense of an adjoining gripping region. Suppose along a contact line between two fibres, the region $x^{(1)} \leq x \leq x^{(2)}$ is slipping and the region $x^{(2)} \leq x \leq x^{(3)}$ is gripping at a given ε_0. The assumption of elastic–perfectly plastic behaviour requires that the shear traction be continuous at $x = x^{(2)}$. This continuity condition will be further developed in the following section.

DEVELOPMENT OF PERFECT LATTICE MODEL

Consider the perfect repeating lattice of identical fibres exhibited in Figure 3a. The symmetry of this idealized

 Copyright © 2008 The Textile Institute

Downloaded By: [Godfrey, Thomas A.] At: 13:54 28 January 2008

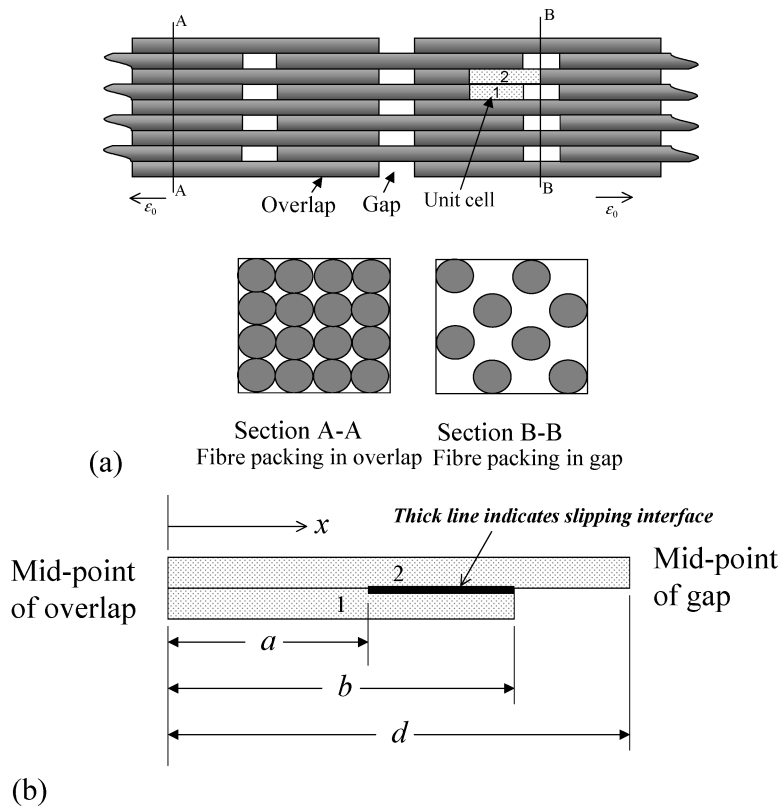

Figure 3 (a) Perfect lattice fibre bundle. (b) Unit cell.

geometry makes a closed-form symbolic solution feasible. The number of neighbouring fibres (coordination number), m, is shown as four in Figure 3a, indicating square packing. A unit cell is exhibited in Figure 3b, and the location of the unit cell in the fibre bundle lattice is identified in Figure 3a. The unit cell is placed so that the origin is at the midpoint of the fibre-to-fibre overlap, and the end of the unit cell is at fibre 2 midpoint.

The fibres are modeled as uniform linear elastic rods loaded by surface shear tractions arising from interactions with abutting fibres. The fibre load-displacement relation is given by

$$p_n = \mathrm{EA}\frac{du_n}{dx} \tag{2}$$

where $p_n(x)$ denotes the axial load in the nth fibre, EA is the fibre extensional stiffness, and du_n/dx is the axial strain in fibre n.

Force equilibrium of fibres in lattice

The unit cell is divided into region I ($0 \le x < a$), region II ($a \le x < b$), and region III ($b \le x < d$), where, respectively, abutting fibre surfaces grip, slip, and fibre surfaces do not make contact. In what follows, the force equilibrium equations will be developed for the three regions.

In region I, fibre 1 grips m abutting fibres. The m abutters have the same displacement as fibre 2 in the unit cell. Shear tractions on fibre 1 from the abutting fibres are written using Equation (1), where it is assumed that the contributions from each abutter may be superposed. Using Equation (2), axial force equilibrium on a differential element of fibre 1 may be written as

$$\mathrm{EA}\frac{d^2u_1}{dx^2} + mk(u_2 - u_1) = 0. \tag{3}$$

Similarly, m abutters grip fibre 2, each abutter having the displacement of fibre 1. Equilibrium of fibre 2 is given by

$$\mathrm{EA}\frac{d^2u_2}{dx^2} + mk(u_1 - u_2) = 0. \tag{4}$$

In region II, slip occurs along the interface. The slip traction acts in the positive direction on fibre 1 and in the negative direction on fibre 2. Therefore, the equilibrium equations become

$$\mathrm{EA}\frac{d^2u_1}{dx^2} + mq_s = 0 \tag{5}$$

and

$$\mathrm{EA}\frac{d^2u_2}{dx^2} - mq_s = 0. \tag{6}$$

Copyright © 2008 The Textile Institute

Downloaded By: [Godfrey, Thomas A.] At: 13:54 28 January 2008

The second fibre is alone in region III, without surface tractions from neighbouring fibres. Therefore, we have

$$\frac{d^2u_2}{dx^2} = 0. \tag{7}$$

Boundary and continuity conditions

The lattice is extended to nominal strain ε_0, resulting in a nominal strain of ε_0 in the periodic unit cell. As such, a displacement boundary condition, written as

$$u_2(d) = \varepsilon_0 d, \tag{8}$$

is used to extend the unit cell.

At the origin, symmetry implies that tensions in fibres 1 and 2 must be the same. In addition, while individual fibre displacements are permitted at the origin, no overall (average) displacement of the assembly may occur. These conditions may be written as

$$p_1(0) = p_2(0) \tag{9}$$

and

$$u_1(0) = -u_2(0). \tag{10}$$

Fibre 1 has a stress-free end at $x = b$. We require that the strain vanish at that point, therefore,

$$\left.\frac{du_1}{dx}\right|_{x=b} = 0. \tag{11}$$

Both fibres are continuous at $x = a$; therefore, fibre displacements and strains are continuous across the boundary of regions I and II ($x = a$). In addition, the shear traction is continuous across the boundary between the gripping and slipping region, that is, regions I and II. Fibre 2 has continuous displacement and strain across the boundary of regions II and III ($x = b$). These continuity conditions may be written as

$$u_i^{\mathrm{I}}(a) = u_i^{\mathrm{II}}(a),\ \left.\frac{du_i^{\mathrm{I}}}{dx}\right|_{x=a} = \left.\frac{du_i^{\mathrm{II}}}{dx}\right|_{x=a}, \quad i = 1, 2, \tag{12}$$

$$q_s = k\left\{u_2^{\mathrm{I}}(a) - u_1^{\mathrm{I}}(a)\right\}, \tag{13}$$

$$u_2^{\mathrm{II}}(b) = u_2^{\mathrm{III}}(b) \quad \left.\frac{du_2^{\mathrm{II}}}{dx}\right|_{x=b} = \left.\frac{du_2^{\mathrm{III}}}{dx}\right|_{x=b}, \tag{14 a,b}$$

where Roman numeral superscripts refer to the displacement solution in the respective region.

Nondimensionalization

Dimensionless position coordinate and displacement variables are introduced, defined by

$$x = \sqrt{\mathrm{EA}/mk}\,\xi,\ u_i = \varepsilon_0\sqrt{\mathrm{EA}/mk}\,U_i, \quad i = 1, 2. \tag{15 a,b}$$

Equations (15a) and Equations (15b) are substituted into the governing equations, yielding are nondimensional forms. Equilibrium equations, by region, become

region I

$$U_1'' + U_2 - U_1 = 0, \quad U_2'' + U_1 - U_2 = 0, \tag{16}$$

region II

$$U_1'' + Q_s = 0, \quad U_1'' - Q_s = 0, \tag{17}$$

region II

$$U_2'' = 0, \tag{18}$$

where primes denote differentiation with respect to ξ and $Q_s = \frac{q_s}{\varepsilon_0}\sqrt{m/k\mathrm{EA}}$.

The boundary and continuity conditions become

$$U_2(\bar{d}) = \bar{d}, \tag{19}$$

$$U_1'(0) = U_2'(0), \quad U_1(0) = -U_2(0), \tag{20a,b}$$

$$U_1'(\bar{b}) = 0, \tag{21}$$

$$U_i^{\mathrm{I}}(\bar{a}) = U_i^{\mathrm{II}}(\bar{a}), \quad U'^{\mathrm{I}}_i(\bar{a}) = U'^{\mathrm{II}}_i(\bar{a}), \quad i = 1, 2, \tag{22 a,b}$$

$$Q_s = U_2^I(\bar{a}) - U_1^I(\bar{a}), \tag{23}$$

$$U_2^{II}(\bar{b}) = U_2^{III}(\bar{b}),\ U'^{II}_2(\bar{b}) = U'^{III}_2(\bar{b}), \tag{24}$$

where the dimensionless parameters $\bar{a}$, $\bar{b}$, and $\bar{d}$ are defined, using Equation (15a), as $(a, b, d) = \sqrt{\mathrm{EA}/mk}(\bar{a}, \bar{b}, \bar{d})$. In the dimensionless position coordinate, regions I through III are defined as $0 \le \xi < \bar{a}$, $\bar{a} \le \xi < \bar{b}$, and $\bar{b} \le \xi < \bar{d}$, respectively.

Solution in each region

The solution in region I is accomplished by writing the system of equations, that is, Equations (16a) and (16b), in matrix form and adopting an eigenvector expansion approach, as illustrated for a similar boundary value problem by Godfrey and Rossettos (1999). The solution is written as

$$U_1^{\mathrm{I}} = C_1\exp(-\sqrt{2}\xi) + C_2\exp(\sqrt{2}\xi) + C_3\xi + C_0 \tag{25}$$

$$U_2^{\mathrm{I}} = -C_1\exp(-\sqrt{2}\xi) - C_2\exp(\sqrt{2}\xi) + C_3\xi + C_0. \tag{26}$$

The system has a zero eigenvalue, which leads to the "rigid body" displacement term C_0, and an eigenvalue of $\lambda^2 = 2$, resulting in the exponential terms. The term $C_3\xi$ is a particular solution, which is required to satisfy continuity conditions at $\xi = \bar{a}$.

 Copyright © 2008 The Textile Institute

Downloaded By: [Godfrey, Thomas A.] At: 13:54 28 January 2008

The solutions in regions II and III are obtained easily, and written as

$$U_1^{\mathrm{II}} = -\frac{1}{2}Q_s\xi^2 + C_4\xi + C_5 \tag{27}$$

$$U_2^{\mathrm{II}} = \frac{1}{2}Q_s\xi^2 + C_6\xi + C_7 \tag{28}$$

$$U_2^{\mathrm{III}} = C_8\xi + C_9. \tag{29}$$

The 10 integration constants and parameter Q_s in the solutions, Equations (25)–(29), are determined to satisfy the 11 continuity and boundary conditions, Equations (19)–(24).

PHYSICALLY MEANINGFUL VALUES OF DIMENSIONLESS LENGTH PARAMETERS

We assume that the shearing constant k is approximately equal to the fibre shear modulus, $k \approx G_{\mathrm{LT}}$. Actually, k will be somewhat less than G_{LT} because k reflects the deformation of abutting fibres along a contact line and the combined structure is not as rigid as a perfect block of material in homogeneous shear. Using the nondimensionalization scheme, making the substitution $A = \pi D^2/4$ for circular fibres, where D is the fibre diameter,

$$(\bar{a}, \bar{b}, \bar{d}) \approx \frac{m}{\pi^{1/2}} D^{-1} \left(\sqrt{E/G_{\mathrm{LT}}}\right)^{-1} (a, b, d). \tag{30}$$

Values of E/G_{LT} range from 5 to 50 for most textile fibres, with higher values for high-strength fibres, up to about 300 for poly p-phenylene-2,6-bezobisoxazole (PBO). Therefore, taking m to be 4, the value of the scale factor $\frac{m}{\pi^{1/2}}(\sqrt{E/G_{\mathrm{LT}}})^{-1}$ is in the range of 0.1–1.0. Staple length is approximately four d in the model, so for proper order of magnitude we take d to be $\sim 10^{-2}$ m, and D to be $\sim 10^{-5}$ m. Therefore, $d/D \sim 1000$. Using Equation (30), with the scale factor and d/D estimates, values of $\bar{d}$ may be seen to range from 100 to 1000. Considering the likelihood that $k < G_{\mathrm{LT}}$, we extend the lower end of the range down to 50.

RESULTS AND DISCUSSION

Fibre strain profiles in perfect lattice and shifted lattice models

The strain in fibre 2 is exhibited in Figure 4 for the case of $\bar{d} = 50$, $\bar{b} = 40$, and $\bar{a}$ values of 30, 35 and 40, respectively. The strain profile is symmetric about the fibre midpoint; only the left half of the profile is shown in the figure. Noting that slip region length is $\bar{b} - \bar{a}$, higher values of $\bar{a}$ correspond to shorter slip regions near fibre tips, where the $\bar{a} = 40$ case represents a completely nonslipping interface. Increasing fibre-to-fibre slip region extent is seen to decrease peak strains and lengthen the strain recovery regions near fibre tips. In all cases, strain in the nonoverlapping fibre region is two times the strain in the overlapped region. This is a consequence of the packing of fibres in the lattice, where the packing density is twice as high in the overlapped versus nonoverlapped regions (see Fig. 3a).

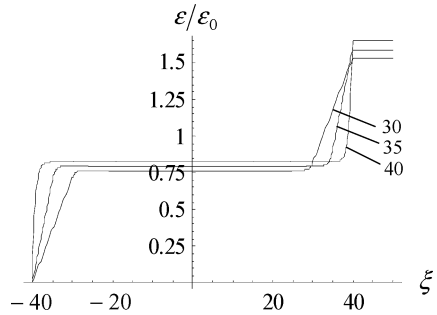

Figure 4 Strain in fibre 2, perfect lattice model, $\bar{d} = 50$, $\bar{b} = 40$, and $\bar{a}$ values as indicated.

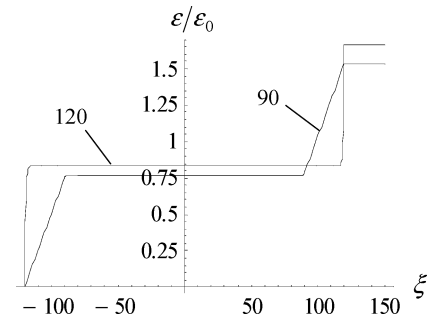

Figure 5 Strain in fibre 2, perfect lattice model, $\bar{d} = 150$, $\bar{b} = 120$, and $\bar{a}$ values as indicated.

The fibre 2 strain profiles for $\bar{d} = 150$, $\bar{b} = 120$, and $\bar{a}$ values of 90, and 120 (nonslip) are shown in Figure 5. At these larger values of dimensionless length, the curves are seen to exhibit sharper corners compared with the $\bar{d} = 50$ results. This can be understood through the elastic shearing mechanism of load transfer and the nondimensionalization scheme. Higher values of $\bar{d}$ for a given physical length d result from increasing values of the ratio of shear stiffness to axial stiffness, that is, mk/EA. As shear stiffness increases relative to axial stiffness, elastic load transfer occurs over a shorter physical length of abutting fibre contact line and axial strains change rapidly along the fibre length. Note that an increased value for m, to, say, six for closest packing, has the same effect as increased shear stiffness. Therefore, we see nearly step function behaviour in the strain profile for the completely nonslipping case and sharp corners in the partially slipping case. In particular, for the partially slipping case, the elastic load transfer mechanism can be neglected entirely—the fibre strain profile is essentially identical to that obtained for the simple assumption that all shear tractions occur in the slipping regions.

In actual fibre bundles, fibre ends are nearly uniformly distributed along the bundle length. In contrast, the complete alignment of fibre ends present in the perfect lattice unit cell results in the extremely high concentration of

Copyright © 2008 The Textile Institute

Downloaded By: [Godfrey, Thomas A.] At: 13:54 28 January 2008

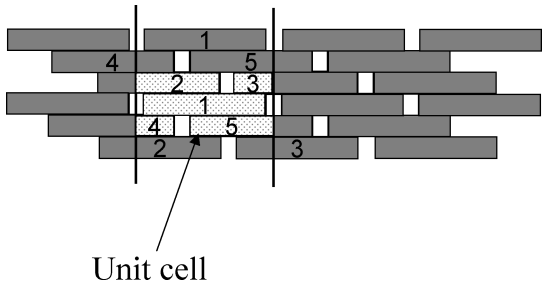

Figure 6 Shifted lattice fibre bundle.

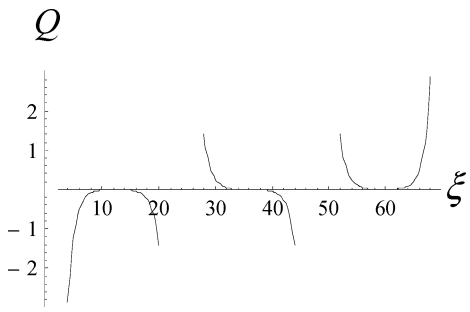

Figure 7 Total dimensionless shear force on fibre 1, shifted lattice model.

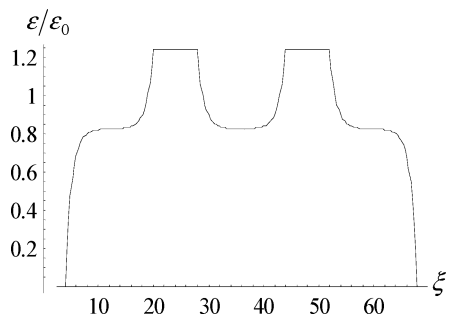

Figure 8 Fibre strain profile, shifted lattice model.

strain in the nonoverlapping region, $\bar{b} < \xi < \bar{d}$, as discussed previously. For a better approximation of actual fibre strain profiles, we consider a slightly more complex fibre arrangement, which we denote as the shifted lattice model, where the ends of abutting fibres occur toward the tips of a given fibre, and where abutting fibres run in both directions, that is, toward the tip and toward the fibre midpoint. This fibre arrangement is depicted in Figure 6. To keep the mathematical treatment of this geometry simple, only elastic interactions between the abutting fibres are permitted, as in Equation (1), and the geometry considered is essentially two dimensional—the layer of fibres depicted in Figure 6 is one of many identical layers assembled in a square-packed bundle. For conciseness, the mathematical development will not be given, as it follows closely that of the perfect lattice model. As the solution for this geometry involves 33 integration constants, the system will be solved numerically.

The total shear force profile along fibre 1 is exhibited in Figure 7 for the case of fibres with a staple length of 64 in the dimensionless length units. Somewhat longer staple lengths may be more physically reasonable; however, numerical problems are encountered due to matrix ill-conditioning. The total shear force is given in dimensionless form as $Q_T = \frac{\sum q_{1,i}}{\varepsilon_0}\sqrt{m/k\mathrm{EA}}$, where the $q_{1,i}$ are the shear tractions on fibre 1 arising from the ith abutting fibre, given by Equation (1), and the shear tractions are summed over the abutting fibres at particular ξ coordinate positions. The large negative shear force on the fibre's left end and positive shear force on the fibre's right end act to extend the fibre and are due to the proximity of the tips of fibre 1. The smaller shear forces occur due to the tips of the abutting fibres 4, 5, 2, and 3 in order of increasing ξ. Right end fibre tips exert negative shears and left end tips exert positive shears on fibre 1. Since the bundle geometry features successive right and left end tips abutting fibre 1, the fibre is subjected to what are essentially self-equilibrating groups of shear tractions that lead to localized strain fluctuations. The fibre strain profile is exhibited in Figure 8. Strain is seen to rapidly recover at the fibre ends and displays maximum plateaus in the gap areas between the tips of abutting fibres. Due to the periodicity of the gap areas in the lattice, these strain maximums are significant, though not as great is in the perfect lattice model.

Fibre strain profiles in realistic (nonperiodic) fibre bundles

As mentioned above, we expect nearly uniform distribution, and little coherence, of fibre end position in actual fibre bundles. Therefore periodic, lattice-type structures (like those investigated here) will tend to overestimate the influence of the ends of abutting fibres on the strain profile in a given fibre. In addition, we expect the fibre ends abutting a given fibre to be nearly evenly divided between ends that will exert positive shears and ends that will exert negative shears, similar to the effects seen in the shifted lattice model discussed above. The combination of uniform end distribution and equal likelihood of left and right ends will tend to smooth out strain fluctuations along the fibre outside of its own end-affected regions. Calculations of strain concentrations in bundles of *continuous* fibres near isolated breaks give a good indication of the approximate size of strain fluctuations in realistic staple fibre bundles. In square-packed bundles of like fibres, strains in a fibre abutting a break are increased by 14% or less (Rossettos and Godfrey, 2002). The maximum of 14% applies for no slip along the abutting interface—the presence of slip will significantly reduce the strain concentration.

In view of the preceding argument, a relatively flat distribution of strain over the middle portion of the fibre may be expected. In addition, given the large sizes of the dimensionless length parameters estimated from typical staple fibre lengths and mechanical properties, we may assume that generally fibre strain profiles will exhibit straight line strain recovery from the ends, and for the case of little or no slip, the strain profile will exhibit nearly step function like behaviour. These points taken together, therefore, indicate

 Copyright © 2008 The Textile Institute

Downloaded By: [Godfrey, Thomas A.] At: 13:54 28 January 2008

that the *short fibre composite model* (Fig. 1) provides an excellent approximation for fibre stress or strain distribution in actual fibre bundles.

Fibre motion in macroscopically homogeneous bundle extension

It appears that the results here suggest each fibre is pulled away from each of its abutters, in violation of the notion that, in real bundles, two or more fibres in contact may move in the same direction. Actually, although there are interfibre shear forces that indicate mutual pulling away, abutting fibres are essentially moving together. The models have been derived to simulate macroscopically homogeneous deformation, that is, the nominal strain is uniform along the length of the bundle. Near fibre tips there is always relative displacement between fibres and associated shear forces; however, in physical terms these relative displacements are small, and indeed, where the abutting fibres are not slipping, relative displacements are much less than a fibre diameter. As such, to a first approximation, all fibres move together such that the gross total displacement of each fibre at a given x position in the bundle is nearly the same. It should be noted that the shear force distributions and fibre strain profiles here, while obtained for very idealized bundle geometries, arise, nonetheless, from the solution of a boundary value problem where realistic assumptions are made regarding interfibre constitutive behaviour and boundary conditions. If, in our analysis, we were to consider macroscopically inhomogeneous extension of a bundle that is not *self-locking*, a point is reached during extension where a completely slipping interface develops between two subsections of the bundle. As remote extension of the bundle continues, the bundle slips apart locally leading eventually to rupture. During this localized deformation, individual fibres move either in the $-x$ or $+x$ direction (depending on subsection), and except for fibres lying directly on the slipping interface, each fibre moves along with it abutters.

Growth of slipping regions with increasing strain

In this section, we use the perfect lattice model to investigate the growth of slipping regions with increasing bundle strain.

The perfect lattice model is sufficiently simple to solve symbolically (*MATHEMATICA*® was used here). The parameter Q_s is found to be

$$Q_s = \frac{2\bar{d}\{1+\exp(2\sqrt{2}\bar{a})\}}{\left\{\begin{array}{l} 1+\sqrt{2}\bar{a}+\bar{a}^2-\bar{b}^2-2\sqrt{2}\bar{d}- \\ 4\bar{a}\bar{d}+4\bar{b}\bar{d}+\exp(2\sqrt{2}\bar{a}) \\ (1-\sqrt{2}\bar{a}+\bar{a}^2-\bar{b}^2+2\sqrt{2}\bar{d}- \\ 4\bar{a}\bar{d}+4\bar{b}\bar{d}) \end{array}\right\}} \tag{31}$$

Permissible values of $\bar{a}$ are such that $0 \le \bar{a} \le \bar{b}$, encompassing the range of initial onset of slip from a nonslipping state$\left(\bar{a} \to \bar{b}^-\right)$, partial slip$\left(0 < \bar{a} < \bar{b}\right)$, and the onset of complete slip$\left(\bar{a} \to 0^+\right)$ along the fibre-to-fibre interface. A key value of Q_s is that associated with the initiation of slip, denoted Q_{IS}. Setting $\bar{a} = \bar{b}$ and assuming reasonable parameter values, a very good approximation for Q_{IS} is obtained by discarding small terms (without the exponential factor),

$$Q_{\mathrm{IS}} \cong \frac{2\bar{d}}{1-\sqrt{2}\bar{b}+2\sqrt{2}\bar{d}}. \tag{32}$$

The parameter Q_{IS} is seen to be $O(1)$ for reasonable parameter values $\left(\bar{b}, \bar{d} \gg 1\right)$.

The parameter Q_s may be interpreted as a nondimensional frictional slip "strength" at the fibre-to-fibre interface. Values of $Q_s > Q_{\mathrm{IS}}$ pertain to bundles under conditions such that no slip occurs—the interface is too strong. The definition of Q_s includes the constants m, k, EA, and the quantities q_s and ε_0. The value of ε_0 will, of course, increase monotonically during the extension process, and the physical slip frictional force per length, q_s, is regarded as a function of ε_0. The function $q_s(\varepsilon_0)$ will depend on fibre frictional properties and on the lateral pressure exerted on the fibre bundle.

Consider the special case of $q_s =$ constant, as might represent the behaviour of fibres that have been given a surface treatment, for example, an adhesive coating. Recalling the definition of Q_s, we may identify a value of the nominal bundle strain that corresponds to the onset of slip, $\varepsilon_{0\mathrm{IS}} = q_s/Q_{\mathrm{IS}}\sqrt{m/k\mathrm{EA}}$. An increased coordination number, m, will lead to a reduction in $\varepsilon_{0\mathrm{IS}}$, whereas increased k and EA lead to increases in the nominal strain at onset of slip. Using $\varepsilon_0 = \frac{q_s}{Q_s}\sqrt{m/k\mathrm{EA}}$, it can be seen that $\varepsilon_0/\varepsilon_0 = Q_{\mathrm{IS}}/Q_s$. From the latter relationship, along with Equations (30) and (32), the growth of the slipping region with increasing strain can be determined.

The above approach can be extended to more general behaviour for $q_s(\varepsilon_0)$ by adopting a power law form, $q_s = c\,\varepsilon_0^{1-n}$, similar to the expression introduced by Rossettos and Godfrey (2002). Here, c is a constant with dimensions of force/length, and n takes on fractional values in the range of 0–1. Through the use of this simple empirical formula, we may explore trends in the behaviour of bundles of fibres embedded in staple yarns. The exponent n models the non-Amontons' law behaviour of fibre-to-fibre friction and the increase in lateral stresses in the bundle due to extension. As mentioned earlier, modeling of fibre bundles embedded in twisted yarns is complex; here, we have assumed a uniform lateral stress on the fibre bundle in lieu of the varying lateral stresses occurring in actual yarns due to fibre migration. By making the appropriate substitutions of the power law form in the expressions for Q_{IS} and Q_s, it is easy to show that the strain ratio can be written as

$$\frac{\varepsilon_0}{\varepsilon_{0\mathrm{IS}}} = \left(\frac{Q_{\mathrm{IS}}}{Q_s}\right)^{1/n}. \tag{33}$$

Copyright © 2008 The Textile Institute

Downloaded By: [Godfrey, Thomas A.] At: 13:54 28 January 2008

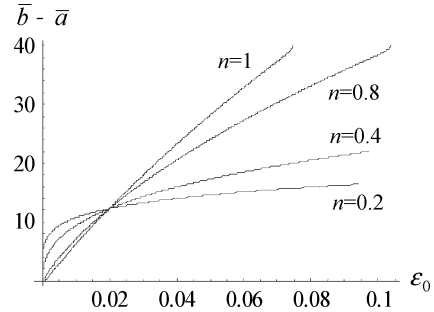

Figure 9 Growth of slip extent, $\bar{b} - \bar{a}$, with increasing strainε_0, $\bar{d} = 50$, $\bar{b} = 40$, and various values of n.

The special case of constant q_s is recovered by setting $n = 1$ in Equation (33). Returning to the definition, $Q_s = \frac{q_s}{\varepsilon_0}\sqrt{m/k\mathrm{EA}}$, a value of $n = 0$ results in Q_s becoming independent of strain, suggesting that under such conditions, the extent of the slip region does not grow with increasing strain.

The growth of slip extent with increasing strainε_0 is exhibited in Figure 9 for the case $\bar{d} = 50$, $\bar{b} = 40$, and various values of n. For this comparison, the c values have been chosen such that q_s is the same in each case at $\varepsilon_0 = 0.02$, and the remaining physical constants are assigned values such that, for $n = 1$, $\varepsilon_{0\mathrm{IS}} = 0.001$. For smaller values of n, slip extent is seen to increase rapidly at small strains, but level off and increase slowly at moderate strains. Therefore, small n values promote self-locking behaviour of the fibre bundle within the yarn. For a linear relationship between yarn lateral pressure and axial extension, and typical fibre power-law friction behaviour (Morton and Hearle, 1975, p. 619), n values of about 0.1–0.3 may be expected (note that the friction index n defined in the reference is a different parameter).

Bundle tension and tangent stiffness

In this section, we use the perfect lattice model to investigate bundle tension and the tangent stiffness of bundles.

The average fibre tension is obtained from the load-displacement relation, Equation (2), evaluated at the origin,

$$p = \varepsilon_0 \mathrm{EA} \frac{du_i}{d\xi}\bigg|_{\xi=0}, \quad i = 1 \text{ or } 2. \tag{34}$$

The average fibre tension with increasing slip extent is exhibited in Figure 10 for the case $\bar{d} = 50$ and $\bar{b} = 40$. The tension p is normalized by the fibre tension in a bundle of continuous (but otherwise identical) fibres under the same nominal strain. In this case, average tension relative to the continuous fibre bundle, $p/\mathrm{EA}\varepsilon_0$, is seen to decrease from 0.82 at initial slip to 0.63 at full slip along the interface. Larger values of the dimensionless length parameters result in similar trajectories as full slip is approached. Normalized average tension at the full slip limit is particularly insensitive to parameter values, for example, the case $\bar{d} = 150$ and $\bar{b} = 120$ also results in a value of $p/\mathrm{EA}\varepsilon_0 = 0.63$;

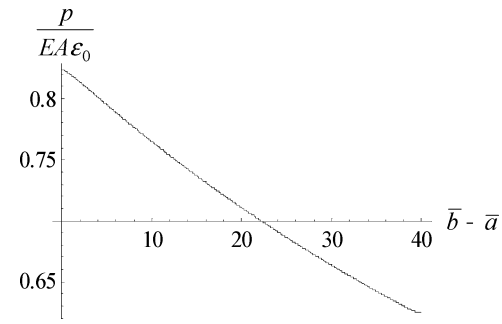

Figure 10 Normalized average tension in bundle with increasing slip extent, $\bar{d} = 50$ and $\bar{b} = 40$.

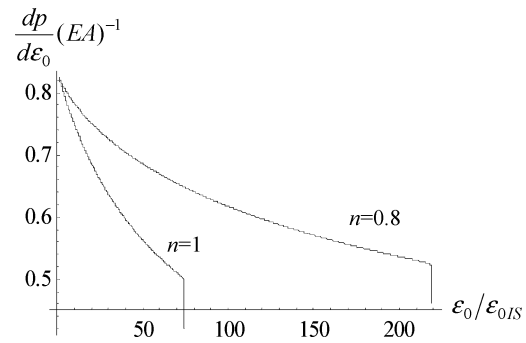

Figure 11 Tangent stiffness of bundle with increasing strain, $\bar{d} = 50$ and $\bar{b} = 40$.

increasing the value of $\bar{b}$ such that $\bar{d} = \bar{b} = 150$, results in $p/\mathrm{EA}\varepsilon_0 = 0.67$. At initial slip, values of normalized average tension approaching one are found for cases with $\bar{d} = \bar{b}$.

A measure of the tangent stiffness of the bundle may be defined as the derivative of the average fibre tension with respect to the nominal strain, $dp/d\varepsilon_0$. Regarding the evaluated derivative in Equation (34) as a function, $f(\gamma)$, where $\gamma \equiv \varepsilon_0/\varepsilon_{0\mathrm{IS}}$, we may write $dp/d\varepsilon_0$ as,

$$\frac{dp}{d\varepsilon_0} = \mathrm{EA}\left(f(\gamma) + \gamma\frac{df}{d\gamma}\right). \tag{35}$$

The behaviour of the tangent stiffness with increasing strain is exhibited in Figure 11 for the cases $n = 1$ and $n = 0.8$, with $\bar{d} = 50$, $\bar{b} = 40$. Starting at roughly 0.8EA, tangent stiffness is seen to decrease moderately with increasing strain to about 0.5EA, at which point the stiffness suddenly drops to nearly 0. The sudden loss of stiffness corresponds to a state of full slip being attained along the fibre–fibre interface. Larger values of the dimensionless length parameters (not shown) stretch the curves out along the $\varepsilon_0/\varepsilon_{0\mathrm{IS}}$ axis.

SUMMARY

In this work, detailed micromechanical models of idealized fibre bundles have been used to investigate fibre strain profiles, slippage behaviour with increasing extension, bundle

 Copyright © 2008 The Textile Institute

Downloaded By: [Godfrey, Thomas A.] At: 13:54 28 January 2008

load-extension, and tangent stiffness properties. The modeling approach permits abutting fibres to interact by elastic surface shear forces arising from fibre shearing deformations in gripping regions and inelastic frictional slip in slipping regions, where transition from gripping to slipping at a contact position occurs as a linear elastic–perfectly plastic function of the interfibre relative displacement. Results show that for typical staple fibre dimensions and physical properties, a short fibre composite model for the fibre strain profile, a constant strain central plateau with straight line strain recovery regions at each end, provides a good approximation to the average fibre strain profile occurring along fibres embedded in bundles. Trends in the self-locking behaviour of fibre bundles in twisted yarns, involving interfibre frictional constitutive behaviour, have been illustrated. For one fibre assembly considered, results for bundle tangent stiffness indicate that, with increasing extension, average bundle stiffness may be expected to decrease from about 0.8 to 0.5 relative to a bundle of similar but continuous fibres, with 0.5 being reached at the point of collapse by localized slippage.

REFERENCES

Godfrey, T. A. and Rossettos, J. N., 1999. The onset of tear propagation at slits in stressed uncoated plain weave fabrics, *J. Appl. Mech.*, 66, 926–933.

Godfrey, T. A. and Rossettos, J. N., 2001. A constitutive model for blended yarn extension with fragmented low-elongation fibres, *Text. Res. J.*, 71, 845–854.

Goswami, B. C., Anandjiwala, R. D. and Carmical, M., 1991. Engineering of fibre properties for spinning on various systems, *J. Appl. Polym. Sci.: Appl. Polym. Symp.*, 47, 463–485.

Hearle, J. W. S., 1965. Theoretical analysis of the mechanics of twisted staple fibre yarns, *Text. Res. J.*, 35, 1060–1071.

Hearle, J. W. S., 1989. In: T.-W. Chou and F. Ko (ed.), *Textile Structural Composites*, Elsevier, Amsterdam, 27–66.

Morton, W. E. and Hearle, J. W. S., 1975. *Physical Properties of Textile Fibres*, Wiley, New York.

Rossettos, J. N. and Godfrey, T. A., 2002. Hybrid effect at fibre breaks in twisted blended yarns, *Text. Res. J.*, 72, 313–319.

Shao, X., Qiu, Y. and Wang, Y., 2005. Theoretical modeling of the tensile behaviour of low-twist staple yarns. Part I: Theoretical model, *J. Text. Inst.*, 96, 61.

Copyright © 2008 The Textile Institute

Downloaded By: [Godfrey, Thomas A.] At: 13:54 28 January 2008

 Copyright © 2008 The Textile Institute